Bioresource Technology 346 (2022) 126574

Contents lists available at ScienceDirect

Bioresource Technology

journal homepage: www.elsevier.com/locate/biortech

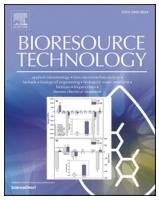

Enhanced biohydrogen production with low graphene oxide content using thermophilic bioreactors

Bhuvan Vemuri [a,b], Vaibhav Handa [a,c], Kalimuthu Jawaharraj [a,b,c,d], Rajesh Sani [b,c,d,e], Venkataramana Gadhamshetty [a,b,c,d,*]

[a] Civil and Environmental Engineering, South Dakota School of Mines and Technology, 501 E Saint Joseph Blvd, Rapid City, SD 57701, USA
[b] BuGReMeDEE Consortium, South Dakota Mines, Rapid City, SD 57701, USA
[c] 2-Dimensional Materials for Biofilm Engineering Science and Technology (2DBEST) Center, South Dakota School of Mines and Technology, SD 57701, United States
[d] Data-Driven Materials Discovery for Bioengineering Innovation Center, South Dakota Mines, 501 E. St. Joseph Street, Rapid City, SD 57701, USA
[e] Chemical and Biological Engineering, South Dakota School of Mines and Technology, SD 57701, United States

HIGHLIGHTS

- Graphene oxide supplement yield 73% pure biohydrogen with 85% conversion efficiency.
- Graphene oxide (GO) supplement resulted in 297% higher biohydrogen yield.
- Acetate fermentation pathway of H_2 production was retained by GO systems.
- Optimal GO levels were identified for thermophilic biohydrogen systems.
- Biodiversity and microbial community biodynamics were evaluated.

ARTICLE INFO

Keywords:
Graphene oxide
Biohydrogen
Thermophiles
Chemical oxygen demand
Nanoparticles

ABSTRACT

Modern society envisions hydrogen (H_2) fuel to drive the transportation, industrial, and domestic sectors. Here, we explore use of graphene oxide nanoparticles (GO NPs) for greatly enhancing bio-H_2 production by a consortium based on *Thermoanaerobacterium thermosaccharolyticum* spp. Thermophilic batch bioreactors were set up at 60 ^{O}C and initial pH of 8.5 to assess the effects of GO NPs supplements on biohydrogen production. Under optimal GO NPs loading of 10 mg/L, the supplemented system yielded ~ 300% higher H_2 yield (6.78 mol H_2/mol sucrose) than control. Such an optimized system offered 73% H_2 purity and 85% conversion efficiency by promoted the desirable acetate fermentation pathway. Miseq Illumina sequencing tests revealed that the optimal levels of GO NPs did not alter the microbial composition of consortium.

1. Introduction

The rapid depletion of fossil fuels and associated environmental problems has been a growing concern to society. Cleaner alternatives to fossil fuels, such as those based on H_2, are urgently needed to alleviate these concerns. H_2 can be used to drive combustion engines and fuel cells to generate heat and electricity, respectively. Water is the sole byproduct in both these processes (Prabakar et al., 2018). Its lower heating value (LHV) is four times higher than coal, gasoline, and methane, respectively. Bioprocesses including photofermentation, microbial electrolysis, photolysis, and dark fermentation can generate H_2 from waste and wastewater sources. Among these four processes, dark fermentation is beneficial because it does not require any external sources of energy inputs (Kumar et al., 2019; Prabakar et al., 2018).

Gram-positive bacteria (e.g., *Clostridia* spp.) use biological pathways to generate hydrogen via fermentation pathways (herein termed as bio-H_2). Volatile fatty acids and carbon dioxide are typical byproducts during bio-H_2 production. The acetate fermentation pathway results in the highest theoretical value of hydrogen yield (eight moles bio-H_2 per mole sucrose). Nearly 60–75% of this yield can be achieved practically by optimizing temperature, pH, and concentration of substrates, micronutrients, and trace elements (Wang and Wan, 2009). Thermophilic (40–65 °C) and hyperthermophilic conditions (>80 °C) can further accelerate bioreaction kinetics, reduce viscosity, improve mixing

* Corresponding author.
E-mail address: Venkata.Gadhamshetty@sdsmt.edu (V. Gadhamshetty).

https://doi.org/10.1016/j.biortech.2021.126574
Received 22 October 2021; Received in revised form 9 December 2021; Accepted 12 December 2021
Available online 16 December 2021

efficiency, reduce risk of contamination and suppress the interference from competing microorganisms such as methanogens (Rittmann and Herwig, 2012). Thermophilic conditions can also assist with the digestion of complex sugars (cellulose, prairie cordgrass) (Bibra et al., 2018; Rittmann and Herwig, 2012; Vemuri et al., 2021).

The current study builds upon the earlier efforts for enabling thermophilic fermentative treatment of dilute municipal wastewater (Vemuri et al., 2021). Our earlier study demonstrated the use of a thermophilic consortium based on *T. thermosaccharolyticum* for removing a significant fraction (~75%) of chemical oxygen demand (COD) from municipal wastewater (COD_{ln} = 200 mg/L) under anaerobic conditions (Vemuri et al., 2021). The current study focuses on using nanoparticles (NPs) for enhancing the bio-H_2 yield by *T. thermosaccharolyticum*. Owing to the unique nanoscale structure and morphological features(Wang and Wan, 2009), nanoparticles offer exceptionally high surface-area-to-volume ratio and biokinetic rates (Contreras et al., 2017; Eroglu et al., 2013; Sekoai et al., 2019). Their crystallinity can also be tuned to control their adsorption capacity and subsequently microbial activity (Haun et al., 2010), specifically by promoting cell attachment, electron transfer pathways, and subsequently biofilm formation (Sekoai et al., 2019).

Nearly, 40% of H_2 is currently generated from natural gas, 30% from naphtha and heavy oil, 18% from coal, and 5% from electrolysis and biomass, respectively (Sinha and Pandey, 2011). Promising biotechnologies including dark fermentation can be used to generate bio-H_2 from renewable biomass. Dark fermentation reduces concerns regarding high energy consumption associated with typical photosynthetic bioreactors. Graphene materials can be used as biocompatible carriers for further improving the performances of dark fermentation process. Reduced graphene oxide (rGO) along with cerium oxide have been used previously to obtain high performance electrodes in microbial electrolytic H_2 production (Pophali et al., 2020). Nickel-graphene composites have been reported to promote bio H_2 production from wastewater (Elreedy et al., 2017; Pugazhendhi et al., 2019). Nanocomposites (Si/$CoFe_2O_4$ and Fe_3O_4/alginate) based on graphene have also been reported to enhance biohydrogen production from lignocellulosic biomass (Srivastava et al., 2019). A majority of prior studies focuses on NPs based on metals and metal oxides, including hematite, nickel oxide, palladium, silver, and copper. Here, we focus on use of pristine form of GO NPs for improving the performance of thermophlic bio-H_2 studies

Owing to biocompatibility, desirable colloidal properties, and large specific surface area, we hypothesize that low levels of GO NPs can promote bio-H_2 production. The current study explores the use of GO NPs for improving bio-H_2 production in thermophilic bioreactors by anaerobic consortium based on *T. thermosaccharolyticum* spp.

2. Materials and methods

Batch fermentation tests (n = 2) were set up to assess the influence of the GO supplementation on bio-H_2 production by the thermophilic consortia. The test reactors varied in the type of GO concentration. Key details on the design of experiments are shown in Table 1.

Table 1
Design of experiments for thermophilic bioprocessing Notes: All tests were carried out at 60 °C and initial pH 8.5.

Reactor	GO (mg/L)	Sucrose (g COD/L)	Heat treated compost, Inocula (g/L)
CP-1	5	10	35
CP-2	10	10	35
CP-3	15	10	35
CP-4	20	10	35
CCP (Control)	0	10	35

CP- Compost test reactor; CCP- Control compost reactor

2.1. Enrichment of thermophilic consortia from heat-treated compost

A 1 cm thick compost sample collected from the Rapid city solid waste facility was heat-shocked at 104 °C for 2 h. The treated sample was cooled to room temperature, sieved with a #50 mesh (300 mm), refrigerated and stored at 4 °C. 35 g of this treated sample was introduced into a 2 L of sucrose supplemented deionized water (COD = 10 g/L) (Rittmann and Herwig, 2012). This mixture was stirred on a magnetic stirrer plate while adjusting its pH to 8.5. The as-prepared solution (175 mL) was transferred into a 250 mL serum bottle. These reactors were capped with butyl rubber septa, crimp sealed, and then the headspace was purged with ultrapure O_2-free N_2 gas using a 22-gauge needle at 15 psi for 15 min. They were continuously stirred at 160 rpm at the test temperature (60 °C). No mineral or vitamin supplements were added. A stock solution of a single-layered GO (6.2 g/L) was prepared for subsequent use. The GO NPs (Graphene Supermarket, Calverton, NY, USA) were characterized by the flake size of 0.5–5 μm, the thickness of ~ 0.34 nm, and composition of 79% carbon and 20% oxygen.

2.2. Miseq Illumina sequencing

Miseq Illumina sequencing was performed on the cultures from the test reactors (exposed to GO) and Controls (no exposure) to determine the composition of the microbial community involved in the bio-H_2 production (Table 2). Here, Illumina 2-step Miseq sequencing was used, which was performed at Research and Testing Laboratory, LLC (Lubbock, TX), to study the microbial diversity among the tested samples. Bacterial biomasses were harvested, and total genomic DNA was extracted using PureLink™ Microbiome DNA Purification Kit (Thermo Fisher Scientific). 16S rRNA gene amplification was performed using this total genomic DNA as the template. PCR was performed in ABI Veriti thermocycler (Applied Biosystems, California). A total of 25 μL reaction was performed using HotStarTaq master mix (Qiagen Inc.) along with 1 μL of forward and reverse primers (5 μM each) and 2 μL of template DNA. The PCR thermal profile is defined below: 95 °C (5 min) and then 35 cycles of 94 °C (30 s), 54 °C (40 s) and 72 °C (1 min), followed by a cycle of 72 °C (10 min) and 4 °C hold. Additionally, a second step Illumina Nextera PCR was performed using i5 index and i7 index sequencing forward and reverse primers, respectively. The same PCR thermal program was followed as listed above except for 10 cycles. Electrolyte Energy Gel (eGel, Life Technologies, Grand Island, New York, United States) was used to analyze the amplified PCR amplicons. Then the PCR amplicons were pooled in equimolar concentration and Solid Phase Reversible Immobilization (SPRI) select reagent (Beckman Coulter, Indianapolis, Indiana) was used to size select from each pool in two rounds in 0.75 ratios for the rounds. Qubit 4 Fluorometer (Life Technologies) was used to quantify the size selected pools and were loaded on an Illumina Miseq (Illumina, Inc. San Diego, California) equipped with 2 × 300 flow cell at 10 pM.

2.3. Membrane protein extraction and quantification

The membrane proteins from the harvested bacteria were extracted using the ReadyPrep Protein Extraction Kit (membrane I) (Bio-Rad Co., Hercules, CA). 10 mL aliquots of the biomass were centrifuged at 8000 rpm and the pellet was used for the protein extraction. Then 0.5 mL of buffer M1 (membrane protein extraction buffer) with 0.05 mL of wet cell pellet was added and mixed gently. This mixture was sonicated on ice with an ultrasonic probe to break open the cells and fragment the genomic DNA. Sonication was performed at 30–40 sec for 15 min. An equal volume of chilled M2 buffer (Membrane protein extraction buffer) was added to the cell extract and vortexed for 30 to 60 sec. These samples were incubated in ice for 10 min. After incubation, the mixtures were incubated at 37 °C for 30 min by mixing the contents in between 3 and 4 times. These samples were centrifuged at 13300 × g for 5 min at room temperature. After centrifugation, the top layer containing the

hydrophilic proteins was transferred to a separate tube. 0.5 mL of the prechilled M2 buffer was added to the bottom layer, vortexed, mixed incubated at 37 °C for 30 min. The samples were again centrifuged at 13300 × g for 5 min at room temperature to extract the remaining hydrophilic protein. The top portion was removed and pooled with the previously extracted hydrophilic protein. The bottom layer containing the hydrophobic proteins was collected separately and quantified using Pierce™ 660 nm Protein Assay reagent (Thermo Scientific, US).

2.4. Analytical methods

A reversible displacement method (RDM) developed in the previous studies was used to release gas pressure and measure gas volume from the test reactors and controls (Gadhamshetty et al., 2009; Rittmann and Herwig, 2012). The same apparatus was used to collect the gas samples (1 mL) from the headspace daily. The gas composition was analyzed using a gas chromatograph (SRI Instruments, model 8610, Torrence, CA) equipped with a thermal conductivity detector (TCD) and a molecular sieve column (Alltech Molesieve 5A 80/100 1.83 m × 38 mm × 26 mm) with argon as carrier gas was used to measure the gas composition. The operational temperatures of the injection port, the oven, and the detector were 100, 70, and 100 °C, respectively. The total volume of the biogas and corresponding hydrogen gas volume for each time interval were determined using the procedures described in the earlier studies (Gadhamshetty et al., 2009; Vemuri et al., 2021). Liquid phase samples were withdrawn and analyzed to measure pH, soluble COD, and VFAs.

A Shimadzu prominence-i LC-2030C plus equipped with UV detector fitted with aminex HPX-87H column was used to identify and quantify acetic acid, butyric acid, and propionic acid. A simple isocratic elution with 0.005 M H_2SO_4 (HPLC grade) was used as a mobile phase to analyze organic acids, all standards, and samples filtered using 0.22 μm syringe filters. A 1 g/L working standard solution was prepared for each organic acid using HPLC grade water. Six calibration levels were prepared via serial dilution of the standard working solution of every organic acid. Separation was performed at 60 °C and at a flow rate of 0.6 mL/min.

3. Results and discussion

3.1. GO NPs effects on bio-H_2 production

The bio-H_2 production increased with an increase in the GO dosage, up to 10 mg/L (Fig. 1). At the end of the test, the CP-2 reactor (GO = 10 mg/L) registered the highest bio-H_2 generation compared to the controls (Fig. 1) with 822 mL. Whereas the three controls, 5 mg/mL, 15 mg/L and 20 mg/L showed biohydrogen production of 249.28 mL, 822 mL, 509.5 mL and 290.3 mL, respectively. These results corroborates with the previous reports where *T. thermosaccharolyticum* generated H_2 as high as 120.05 mL H_2/g of xylan (electron donor) (Saripan and Reungsang, 2013). In another study, T. thermosaccharolyticum yielded ~ 12.08 mmol H_2 g^{-1} Avicel, which was equivalent to 2.17 mol H_2. mol^{-1} glucose (Sheng et al., 2015). Interestingly, genetically engineered *Thermoanaerobacterium aotearoense* (knockouts of e NADH-dependent reduced ferredoxin: NADP + oxidoreductase - NfnAB) enhanced H_2 production from 190 to 209 mmol/L H_2 from corn cob and rice straw hydrolysates that underwent acid pretreatment (Li et al., 2019). The enhanced H_2 production can be well defined by the genetic mechanism of the microbe-GO NPs bio interaction. This involves serval hypotheses including, graphene serving as electron acceptor/acceptor or both in the microbial consortia (Zhang and Tremblay, 2020). Thus, this study hypothesizes that GO NPs are mainly involved in the reduction of GO to rGO. Future research is warranted to depict the exact mechanism or fate of GO NPs on the microbes. In addition, the surface charges of the GO-NPs were measured in different ionic strength solutions (0.1 to 10 mM KCl). The surface charges ranged were −38.60, −40.70, and −45.20 mV at 10, 1, and 0.1 mM, respectively (Hasan et al., 2021). Thus, GO surface

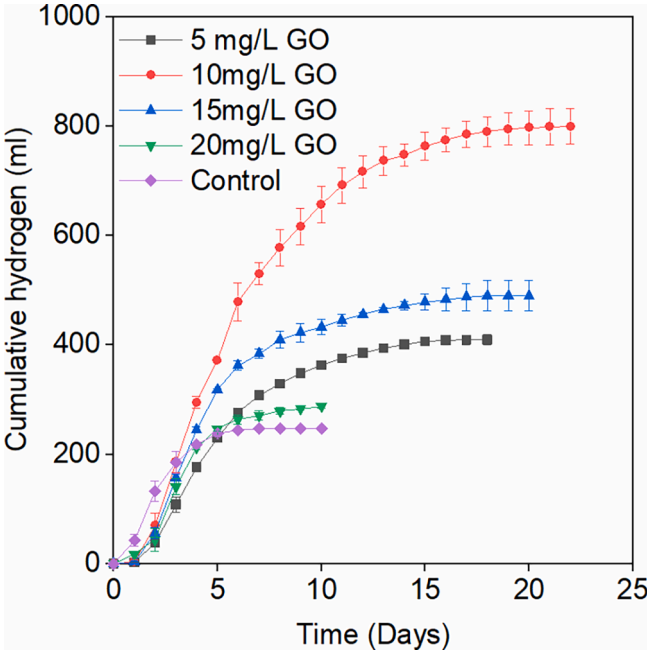

Fig. 1. Cumulative hydrogen production in all 5 reactors (SD < 5%).

charge is expected to be more negative at DI water. In addition, the energy analysis for the biohydrogen production was performed in DF process assuming the hydrogen to electricity conversion efficiency of 65% in a fuel cell. We also assumed that the net energy gain from the volatile fatty acids produced is zero (Vemuri et al., 2021). The results shows that the net energy gain from the DF process using the GO (10 mg/L) as catalyst is 9.11 wh/L. Whereas the net energy gain from the DF without GO addition was calculated to be 2.73 wh/L. Thus, the current system offers nearly 3.3-fold higher energy performance.

The cumulative bio-H_2 production in CP-2 increased by 3.3-fold compared to the control. The H_2 composition of the biogas also increased by 19.3%. The cumulative bio-H_2 production (822 mL) was 230% higher compared to the control without GO NPs inclusion. The cumulative bio-H_2 production at 5 mg/L, 15 mg/L, and 20 mg/L was 416.1 mL, 509.5 mL, and 290.3 mL, respectively. The bio-H_2 production in CP2 lasted for ~ 21 days while that in the control ceased within 10 days. The production lasted for 9, 21, and 19 days in CP1, CP3, and CP4, respectively. As shown in Fig. 2, at 60 °C, these three test reactors achieved peak concentrations of 65.5%, 72.8%, 74.9%, and 67.1%, respectively. These values were greater than the control (~61%) that lacked GO NPs.

The lag phase in the tested reactors (24 to 48 h) lasted longer compared to the control (2–4 h). The longer lag period is attributed to the time required for the consortium to overcome the negative effects of GO on the hydrogenase activity, specifically the undesirable reversible oxidation of bio-H_2. The bacteria-NPs interaction mainly depends on the dosage, hydrophobicity, hydrophilicity, surface chemistry, purity and number of layers (Frontiñán-Rubio et al., 2018; Liao et al., 2018). Graphene NPs exert cytotoxic effects by promoting membrane damage and leakage of cellular contents (Pulingam et al., 2021).

The gas production in control (Fig. 2e) ceased within 8 days of operation, while gas production continued for 17, 20, 18, 10 days in CP1, CP2, CP3, and CP4, respectively (Fig. 2a-d). The enhanced H_2 production can be understood by recognizing the potential for the GO serve as an electron acceptor, specifically to facilitate the mediated electron transfer for enhancing bio-H_2 production (Zhang and Tremblay, 2020). For example, graphene NPs have been reported to promote the electron transfer rates of hydrogenase enzymes responsible for the H_2 fermentation pathway (Elreedy et al., 2017; McPherson and Vincent,

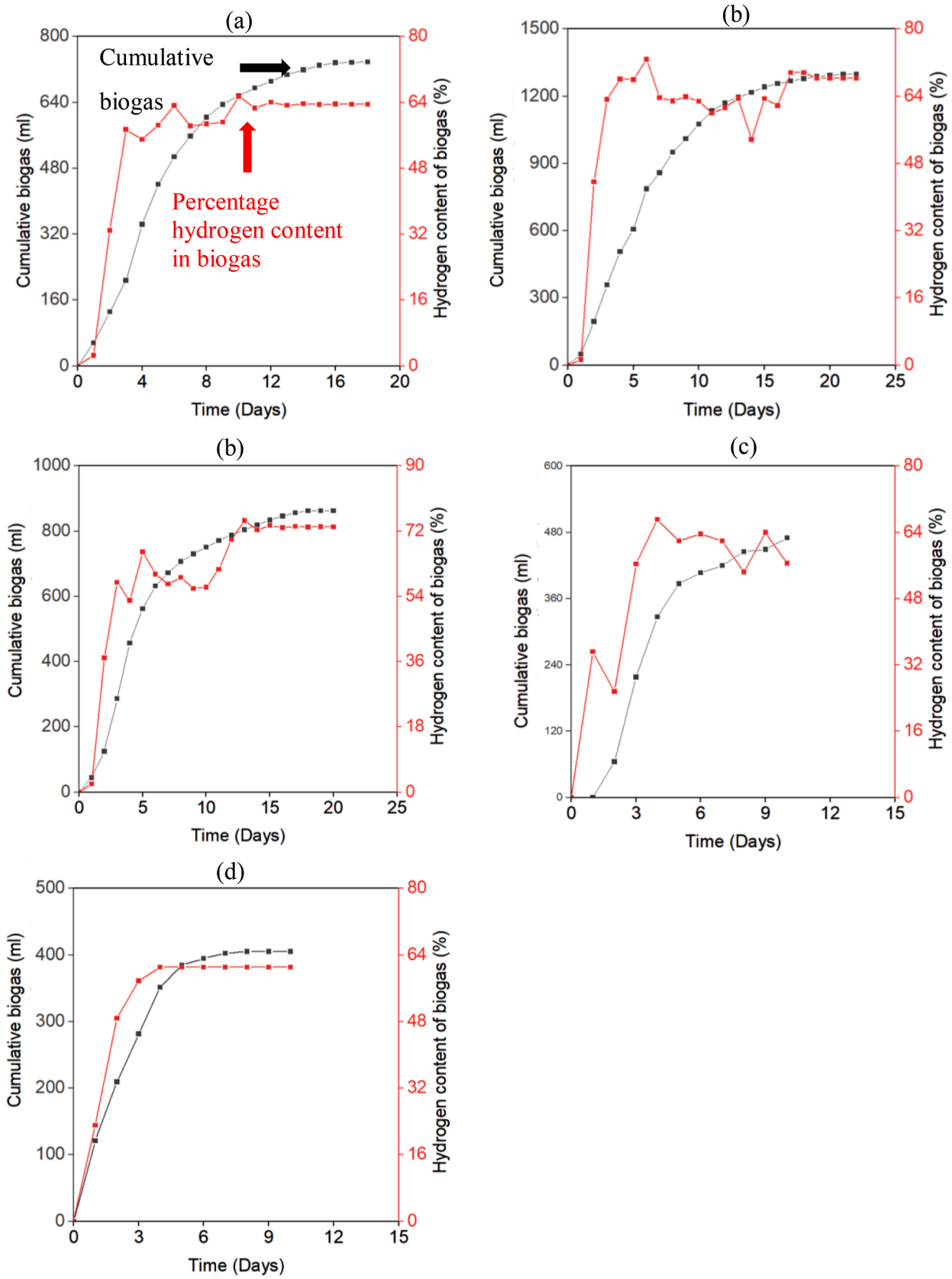

Fig. 2. Hydrogen content in the biogases, and cumulative biogas production in all five reactors (a) CP1 (5 mg/L GO); (b) CP2 (10 mg/L GO); (c) CP2 (15 mg/L GO); (d) CP4 (20 mg/L GO); and (e) CP5 (control).

2014). In addition, certain microorganisms can secrete essential extracellular polymeric substances (EPS) that enhance microbial aggregation to form a physical barrier against the known cytotoxic effects (He et al., 2020; Tawfik et al., 2021). However, beyond the optimal level (10 mg/L), the bio-H_2 production decreased due to the increased oxidative stress by the GO NPs (Liu et al., 2011).

3.2. COD and pH

The initial concentration of sucrose in the test reactors and control was equivalent to 10,000 mg COD/L. At the end of the tests, their COD levels dropped, indicating that sucrose was converted to bio-H_2 (Fig. 3a). The COD in CP2 was reduced by 1540 mg COD/L within 21 days of the test duration. Although the COD removal in the control was 2000 mg COD/L, the volume of bio-H_2 produced was limited to 249.28 mL in 8 days.

The COD removals in CP1, CP3, and CP4 were 1525 mg COD/L, 1570 mg COD/L, and 1370 mg COD/L, respectively. A significant drop in pH was observed in all the reactors (Fig. 3b). This pH drop is due to the accumulation of VFAs and associated bio-H_2 production (Eq 1 & 2). Although the initial pH in all the reactors was set at 8.5, there were slight differences in the pH values at the end of the tests. For example, the pH in CP4 (20 mg GO/L) dropped to 4.11. The pH in the CP1. CP2, CP3, and control reactors dropped to 4.72, 4.61, 4.73, and 5.24, respectively. These differences were also reflected in the amount of VFA accumulation, as explained below.

$$C_{12}H_{22}O_{11} + 9H_20 \rightarrow 4\ C_2H_3O_2^- + 8H^+ + 4HCO_3^- + 8H_2 \quad (1)$$

$$C_{12}H_{22}O_{11} + 5H_20 \rightarrow 2C_4H_8O_2^- + 6H^+ + 4HCO_3^- + 4H_2 \quad (2)$$

3.3. Accumulation of volatile fatty acids

The samples from the test reactors and controls were analyzed for VFAs at the start and end of the experiments (Fig. 4). No VFA peaks were observed at the beginning. However, the acetate peaks appeared in all the reactors at the end. For instance, the acetate levels in CP2 reached 8889.5 mg/L at the end. These results indicate that the sucrose was primarily converted into acetate via the acetate fermentation pathway (Eq. 1). Acetate was the dominant acid in all the other reactors. The acetate accumulation increased with increasing levels of GO until 10 mg/L and then decreased with an increase in GO concentration. The temporal values of the butyrate also followed a similar trend. CP1, CP2, CP3, and CP4 registered butyrate levels of 1044.72, 993.12, 442.33, and 621.05 mg/L, respectively. Generally, thermophilic bio-H_2 reactors generate higher levels of VFAs. Examples can be found in previous studies based on *Thermoanaerobacterium* (Mamimin et al., 2017) and cocultures of *Thermoanaerobacterium* and *Laminaria digitata* (Deng et al., 2022). However, engineered *Thermoanaerobacterium aotearoense* SCUT27 strain (deletion of NADH-dependent reduced ferredoxin:NADP + oxidoreductase (NfnAB)) have been reported to enhance biohydrogen yield by lowering accumulation of lactic acid (Li et al., 2019).

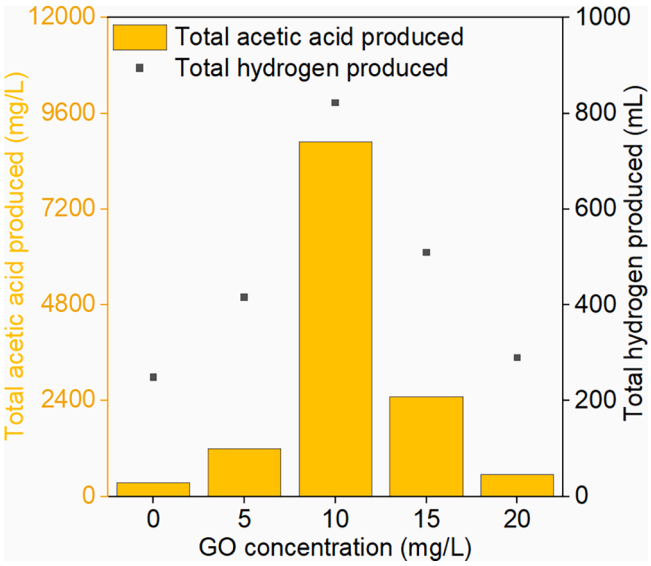

Fig. 4. Comparison of acetate accumulation and bio-H_2 production with changes in GO concentrations.

3.4. Microbial community analysis by Illumina sequencing

The effect of GO NPs on the composition of thermophilic consortia,

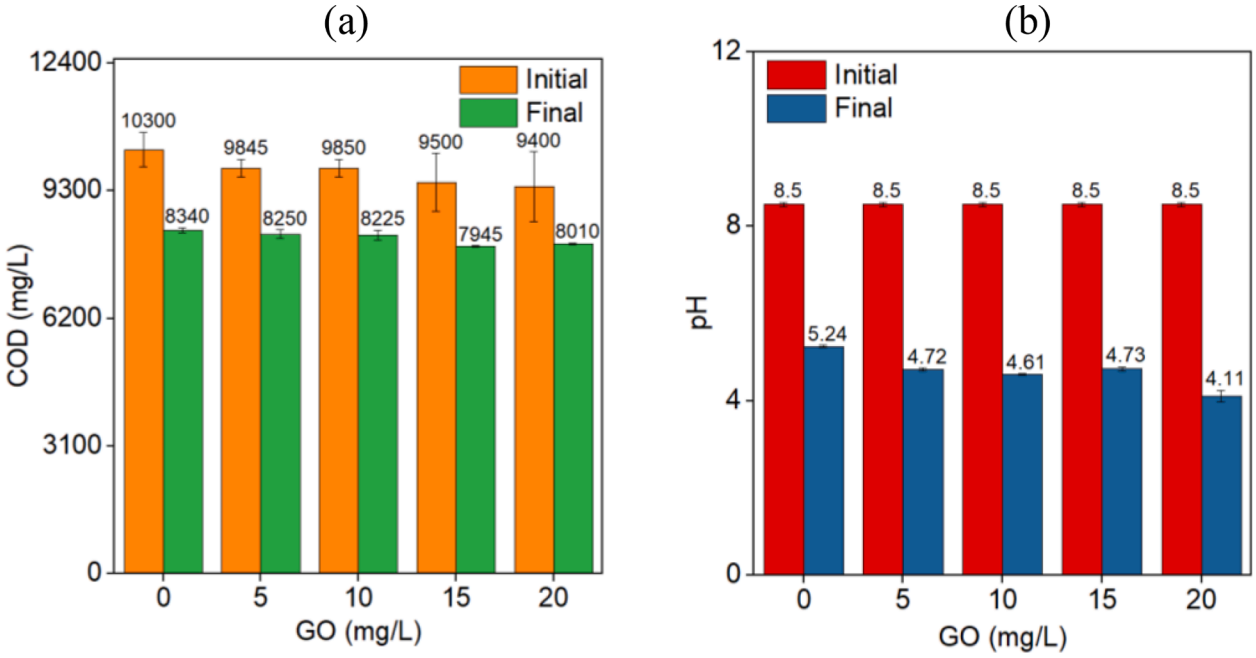

Fig. 3. Changes in (a) COD and (b) pH in all the 5 reactors from initial and final days (error bars indicate SD).

formerly enriched from a thermal hot spring in WY, USA (Bibra et al., 2018; Wang et al., 2018), was evaluated in this study. The relative taxonomic abundance of 16S rRNA gene sequences was compared at the class and the genus level in Figure 5 and Fig. 6, respectively. The community analysis revealed diverse microorganisms among the control, CP2 and CP4 (Figure 5 and 6, respectively). Class level distribution showed that the 10 mg/L GO supplemented reactors were dominated by *Clostridia,* similar to the control. However, the 20 mg/L supplemented cultures yielded other unclassified bacteria (Figure 5). The taxonomic abundance of the control (78%) and 10 mg/L GO (88%) were uniquely dominated by *T. thermosaccharolyticum,* a thermophilic bacterium that was used in the original inocula. This confirms that the 10 mg/L GO system is favoring the enrichment of *T. thermosaccharolyticum.* These findings align with our findings from other studies that reported positive uses of graphene materials in environmental biotechnology applications. Specifically, our earlier studies have demonstrated that metal electrodes modified with graphene materials can enhance the growth of sensitive microorganisms, specifically methanotrophs and methylotrophs in microbial fuel cell applications (Islam et al., 2020; Jawaharraj et al., 2021; Jawaharraj et al., 2020).

T. thermosaccharolyticum, a saccharolytic fermentative thermophilic bacterium, produces hydrogen by degrading cellulose and starch substrates (Saripan and Reungsang, 2013). *T. thermosaccharolyticum* can be expected to be involved in the acetic acid fermentation pathway that utilizes the carbon source in the culture media (Saripan and Reungsang, 2013; Vemuri et al., 2021). This corroborates with the increased acetic acid accumulation (see section 3.1.3) in CP2 that was supplemented with 10 mg/L GO NPs. During both heterotrophic and autotrophic culture modes, *T. thermosaccharolyticum* has been reported to be participating in the "hot" acetogenesis process (Basen and Müller, 2017). The fermentation of sucrose by *T. thermosaccharolyticum* produces organic acids such as acetic acid and butyric acids, resulting in the pH drop (see section 3.1.2), which was observed in all the reactors, including control (Fig. 3b). This result corroborates with a previous report regarding the peak hydrogen production by *T. thermosaccharolyticum* PSU-2 strain using sucrose, starch, and xylose as substrates, respectively (O-Thong et al., 2008).

The initial inoculum used at the beginning of the tests in all the reactors was predominantly *T. thermosaccharolyticum* species (99%). This suggests that the level of GO influences the dynamics of the microbial community structure in control and CP1 compared to other reactors. Also, the control sample yielded other bacteria including *Lysinibacillus* sp. (1%), *Clostridium* sp. (1%) and *Geobacillus thermodenitrificans* (1%). Whereas sample CP1 yielded *Lysinibacillus* sp. (3%), *Clostridium* sp. (1%) and *Geobacillus thermodenitrificans* (1%).

Interestingly, the CP2 reactor with 20 mg/L GO showed more diversity compared to other reactors. This implies that the higher level of GO is favoring non-thermophilic bacteria. *Acinetobacter radioresistens* was found to be the predominant bacteria (35%) among the consortia. None of the earlier studies provided extensive details on GO interaction or the hydrogen production involving *Acinetobacter radioresistens*. In addition, other partnering bacteria were observed in minor quantities. This include *Sphaerobacter thermophilus* (3%), *Bacillus* sp (4%), *Actinomadura* sp (2%), *Geobacillus thermodenitrificans* (2%), *Pseudonocardia* sp. (1%), *Clostridium* sp (1%), *Lysinibacillus* sp (1%), *Thermomonospora chromogena* (1%), *Planifilum fulgidum* (1%), *Micromonospora* sp (0.8%). It is noteworthy to mention that 48.2% of the microbial communities were unidentified. This denotes that excessive GO levels (20 mg/L) are playing a major role in shifting the microbial population when compared to the original inocula.

This hypothesis corroborates with the previous study in which a novel electrogenic bacterium *Desulfuromonas versatilis* was enriched and isolated from GO reducing enrichment culture obtained from the sample mixture based on coastal sand and seawater (Xie et al., 2021). On the

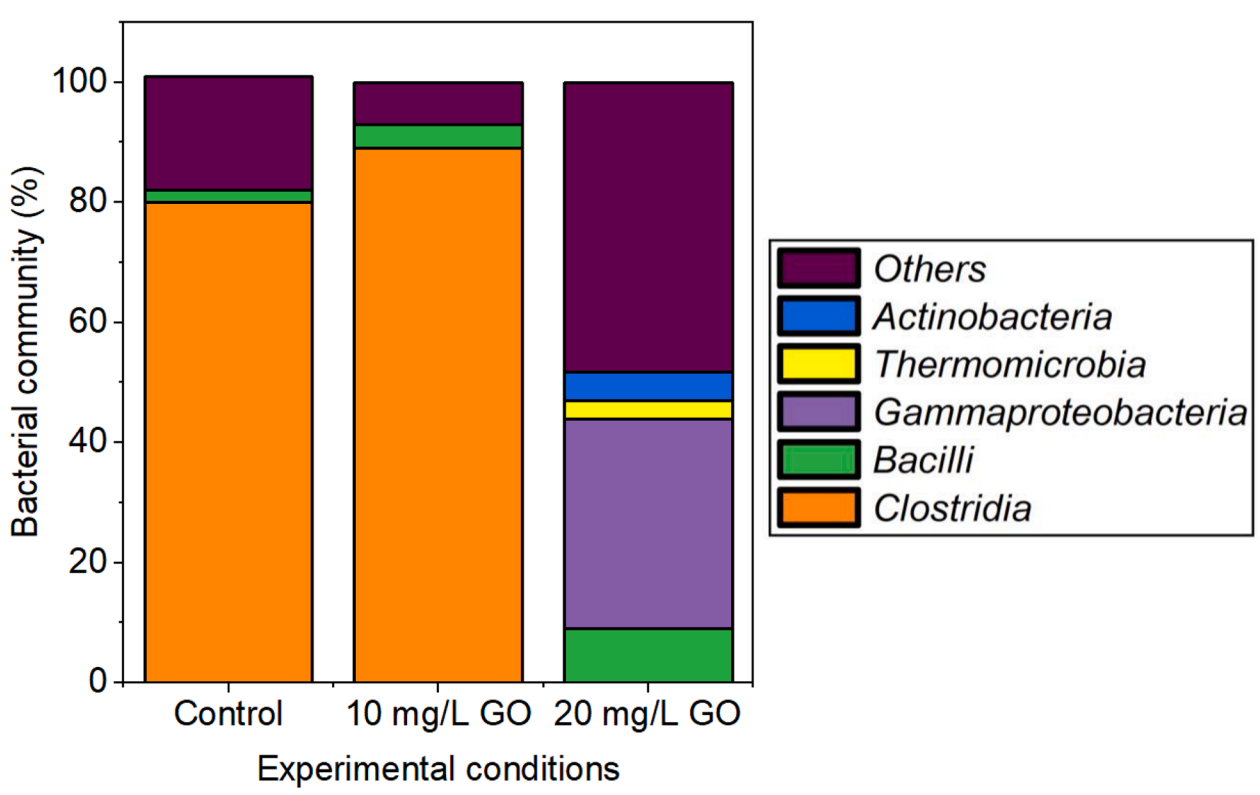

Fig.5. Biodiversity analysis and class level distribution of consortia in the control, 10 mg/L and 20 mg/L supplemented cultures. Percentage of the bacterial communities of control, 10 mg/L and 20 mg/L GO supplemented bacterial cultures showing their class level distribution. Others denote sequences that were assigned to unclassified bacteria.

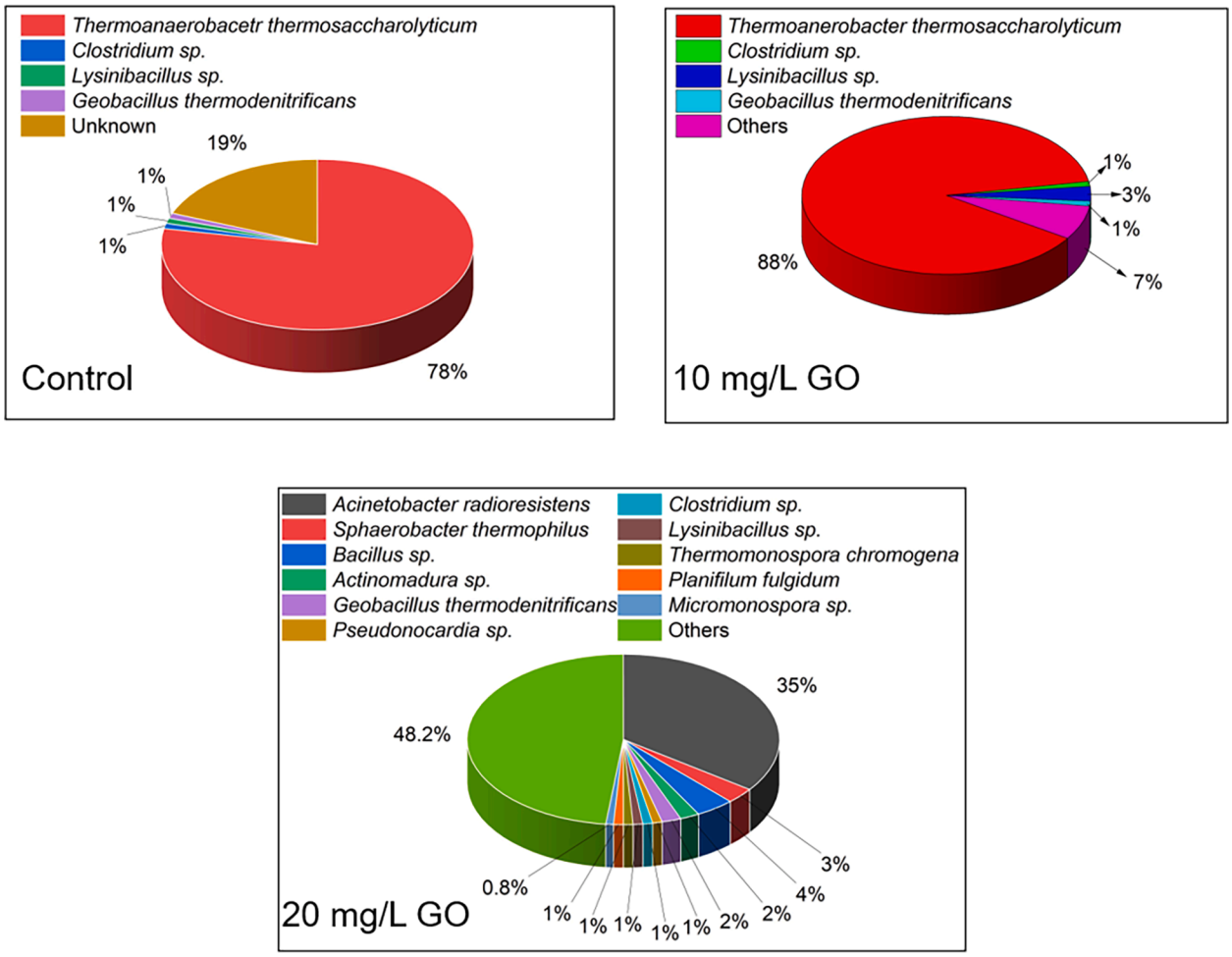

Fig. 6. Biodiversity analysis and genus level distribution of bacterial cultures by Illumina sequencing. The relative taxonomic abundance of 16S rRNA gene sequence and the microbial community analysis of control and 10 mg/L (CP2) supplemented cultures revealed *T. thermosaccharolyticum* as a dominant species. A more diverse community was observed in 20 mg/L supplemented cultures (CP3) with *Acinetobaceter radioresistens* as the predominant bacteria. USEARCH global alignment algorithm was used to run the gene sequences. In addition, the Python program was used to identify the actual assignment. Others denote gene sequences that were allocated to the unclassified bacteria.

other side, GO supplements could elicit microbial toxicity that could adversely affect the growth of select thermophiles (Guo and Mei, 2014). To reduce such adverse toxic effects, surface modification strategies and fabrication methods could be adapted using GO. Future research is warranted to identify the behavioral and evolutionary patterns of microbial consortia exposed to higher levels of GO (>10 mg/L based on this study).

3.5. Membrane protein extraction and quantification

This study hypothesizes that GO NPs interact with bacterial membrane proteins of thermophiles to form a complex membranal structure and enhance bio-H_2. To test this hypothesis, the hydrophobic membrane proteins were extracted, separated and quantified in this study (see supplementary material). The accumulated levels of the membrane proteins in the bio-H_2 reactors ranged between 0.09 and 0.1 g/L when GO NPs remained under 10 mg/L. Whereas the protein concentrations decreased when GO levels increased beyond 10 mg/L (e.g., 0.03 mg/L at 15 mg GO/L). These findings further corroborate that the optimal concentration of GO is 10 mg/L in the current study. The higher levels of GO have favored the enrichment of non-thermophiles (see section 3.1.4). This could be due to the cytotoxic effects exhibited by the graphene nanomaterials on the microbial cell membrane and other cellular structures. A higher degree of exposure to GO has been reported to stimulate the secretion of stress molecules (e.g., reactive oxygen species) that damage the cellular membrane in *E. coli* cells (Qiang et al., 2021). Further studies are warranted to analyze the cytotoxic effects of *Thermoanaerobacterium* spp exposed to GO NPs, especially in terms of their shapes and sizes.

4. Conclusions

This study demonstrated that low levels of GO nanoparticles (10 mg/L) can stimulate the biohydrogen production by ~ 230% in thermophilic batch reactors. The optimal levels of GO supplementation did neither impact microbial community structure nor the metabolic pathways of biohydrogen production. The improved performance offered by GO was attributed to the increased electron flow towards hydrogen production. Further studies are warranted to assess the scalability, technical feasibility, and environmental impacts of GO supplemented systems, especially under flow-through conditions.

CRediT authorship contribution statement

Bhuvan Vemuri: Conceptualization, Validation. **Vaibhav Handa:** Conceptualization, Validation. **Kalimuthu Jawaharraj:** Visualization, Supervision, Resources. **Rajesh Sani:** Project administration. **Venkataramana Gadhamshetty:** Conceptualization, Supervision,

Validation, Project administration, Funding acquisition.

Declaration of Competing Interest

The authors declare that they have no known competing financial interests or personal relationships that could have appeared to influence the work reported in this paper.

Acknowledgments

Authors acknowledge the funding support from National Science Foundation awards (#1849206, 1454102, #1920954, #1736255), Electric Power Research Institute (EPRI #071620), and National Aeronautics and Space Administration (#NNX16AQ98A).

Appendix A. Supplementary data

Supplementary data to this article can be found online at https://doi.org/10.1016/j.biortech.2021.126574.

References

Basen, M., Müller, V., 2017. "Hot" acetogenesis. Extremophiles 21 (1), 15–26. https://doi.org/10.1007/s00792-016-0873-3.

Bibra, M., Kumar, S., Wang, J., Bhalla, A., Salem, D.R., Sani, R.K., 2018. Single pot bioconversion of prairie cordgrass into biohydrogen by thermophiles. Bioresour. Technol. 266, 232–241. https://doi.org/10.1016/j.biortech.2018.06.046.

Contreras, J.E., Rodriguez, E.A., Taha-Tijerina, J., 2017. Nanotechnology applications for electrical transformers—A review. Electr. Power Syst. Res. 143, 573–584. https://doi.org/10.1016/j.epsr.2016.10.058.

Deng, C., Lin, R., Kang, X., Wu, B., Wall, D., Murphy, J.D., 2022. Improvement in biohydrogen and volatile fatty acid production from seaweed through addition of conductive carbon materials depends on the properties of the conductive materials. Energy 239, 122188. https://doi.org/10.1016/j.energy.2021.122188.

Elreedy, A., Ibrahim, E., Hassan, N., El-Dissouky, A., Fujii, M., Yoshimura, C., Tawfik, A., 2017. Nickel-graphene nanocomposite as a novel supplement for enhancement of biohydrogen production from industrial wastewater containing mono-ethylene glycol. Energy Convers. Manag. 140, 133–144. https://doi.org/10.1016/j.enconman.2017.02.080.

Eroglu, E., Eggers, P.K., Winslade, M., Smith, S.M., Raston, C.L., 2013. Enhanced accumulation of microalgal pigments using metal nanoparticle solutions as light filtering devices. Green Chem. 15, 3155–3159. https://doi.org/10.1039/c3gc41291a.

Frontiñán-Rubio, J., Gómez, M.V., Martín, C., González-Domínguez, J.M., Durán-Prado, M., Vázquez, E., 2018. Differential effects of graphene materials on the metabolism and function of human skin cells. Nanoscale 10 (24), 11604–11615.

Gadhamshetty, V., Johnson, D., Nirmalakhandan, N., Smith, G., Deng, S., 2009. Feasibility of biohydrogen production at low temperatures in unbuffered reactors. Int. J. Hydrogen Energy 34 (3), 1233–1243. https://doi.org/10.1016/j.ijhydene.2008.10.037.

Guo, X., Mei, N., 2014. Assessment of the toxic potential of graphene family nanomaterials. J Food Drug Anal. 22 (1), 105–115. https://doi.org/10.1016/j.jfda.2014.01.009.

Hasan, Md., Geza, M., Peterson, J., Gadhamshetty, V., 2021. Graphene oxide transport and retention in biochar media. Chemosphere 264, 128397. https://doi.org/10.1016/j.chemosphere.2020.128397.

Haun, J.B., Yoon, T.-J., Lee, H., Weissleder, R., 2010. Magnetic nanoparticle biosensors. WIREs Nanomed Nanobiotechnol 2 (3), 291–304. https://doi.org/10.1002/wnan.84.

He, C.-S., Ding, R.-R., Chen, J.-Q., Li, W.-Q., Li, Q.i., Mu, Y., 2020. Interactions between nanoscale zero valent iron and extracellular polymeric substances of anaerobic sludge. Water Res. 178, 115817. https://doi.org/10.1016/j.watres.2020.115817.

Islam, J., Chilkoor, G., Jawaharraj, K., Dhiman, S.S., Sani, R., Gadhamshetty, V., 2020. Vitamin-C-enabled reduced graphene oxide chemistry for tuning biofilm phenotypes of methylotrophs on nickel electrodes in microbial fuel cells. Bioresour. Technol. 300, 122642. https://doi.org/10.1016/j.biortech.2019.122642.

Jawaharraj, K., Shrestha, N., Chilkoor, G., Vemuri, B., Gadhamshetty, V., 2020. Electricity from methanol using indigenous methylotrophs from hydraulic fracturing flowback water. Bioelectrochemistry 135, 107549. https://doi.org/10.1016/j.bioelechem.2020.107549.

Jawaharraj, K., Sudha Dhiman, S., Bedwell, S., Vemuri, B., Islam, J., Sani, R.K., Gadhamshetty, V., 2021. Electricity from methane by *Methylococcus capsulatus* (Bath) and *Methylosinus trichosporium* OB3b. Bioresour. Technol. 321, 124398. https://doi.org/10.1016/j.biortech.2020.124398.

Kumar, G., Mathimani, T., Rene, E.R., Pugazhendhi, A., 2019. Application of nanotechnology in dark fermentation for enhanced biohydrogen production using inorganic nanoparticles. Int. J. Hydrogen Energy. 44 (26), 13106–13113. https://doi.org/10.1016/j.ijhydene.2019.03.131.

Li, Y., Hu, J., Qu, C., Chen, L., Guo, X., Fu, H., Wang, J., 2019. Engineered *Thermoanaerobacterium aotearoense* with nfnAB knockout for improved hydrogen production from lignocellulose hydrolysates. Biotechnol. Biofuels 12, 1–14. https://doi.org/10.1186/s13068-019-1559-8.

Liao, C., Li, Y., Tjong, S., 2018. Graphene nanomaterials: Synthesis, biocompatibility, and cytotoxicity. Int. J. Mol. Sci. 19 (11), 3564. https://doi.org/10.3390/ijms19113564.

Liu, S., Zeng, T.H., Hofmann, M., Burcombe, E., Wei, J., Jiang, R., Kong, J., Chen, Y., 2011. Antibacterial activity of graphite, graphite oxide, graphene oxide, and reduced graphene oxide: Membrane and oxidative stress. ACS Nano 5 (9), 6971–6980. https://doi.org/10.1021/nn202451x.

Mamimin, C., Prasertsan, P., Kongjan, P., O-Thong, S., 2017. Effects of volatile fatty acids in biohydrogen effluent on biohythane production from palm oil mill effluent under thermophilic condition. Electron. J. Biotechnol. 29, 78–85. https://doi.org/10.1016/j.ejbt.2017.07.006.

McPherson, I.J., Vincent, K.A., 2014. Electrocatalysis by hydrogenases: Lessons for building bio-inspired devices. J. Braz. Chem. Soc. 25, 427–441. https://doi.org/10.5935/0103-5053.20140042.

O-Thong, S., Prasertsan, P., Karakashev, D., Angelidaki, I., 2008. Thermophilic fermentative hydrogen production by the newly isolated *Thermoanaerobacterium thermosaccharolyticum* PSU-2. Int. J. Hydrogen Energy 33 (4), 1204–1214. https://doi.org/10.1016/j.ijhydene.2007.12.015.

Pophali, A., Singh, S., Verma, N., 2020. Simultaneous hydrogen generation and COD reduction in a photoanode-based microbial electrolysis cell. Int. J. Hydrogen Energy 45 (48), 25985–25995. https://doi.org/10.1016/j.ijhydene.2020.01.053.

Prabakar, D., Manimudi, V.T., Suvetha K, S., Sampath, S., Mahapatra, D.M., Rajendran, K., Pugazhendhi, A., 2018. Advanced biohydrogen production using pretreated industrial waste: Outlook and prospects. Renewable and Sustainable Energy Reviews 96, 306–324. https://doi.org/10.1016/j.rser.2018.08.006.

Pugazhendhi, A., Shobana, S., Nguyen, D.D., Banu, J.R., Sivagurunathan, P., Chang, S. W., Ponnusamy, V.K., Kumar, G., 2019. Application of nanotechnology (nanoparticles) in dark fermentative hydrogen production. Int. J. Hydrogen Energy 44 (3), 1431–1440. https://doi.org/10.1016/j.ijhydene.2018.11.114.

Pulingam, T., Thong, K.L., Appaturi, J.N., Lai, C.W., Leo, B.F., 2021. Mechanistic actions and contributing factors affecting the antibacterial property and cytotoxicity of graphene oxide. Chemosphere 281, 130739. https://doi.org/10.1016/j.chemosphere.2021.130739.

Qiang, S., Li, Z., Zhang, L., Luo, D., Geng, R., Zeng, X., Liang, J., Li, P., Fan, Q., 2021. Cytotoxic effect of graphene oxide nanoribbons on *Escherichia coli*. Nanomaterials 11, 1–12. https://doi.org/10.3390/nano11051339.

Rittmann, S., Herwig, C., 2012. A comprehensive and quantitative review of dark fermentative biohydrogen production. Microb. Cell Fact. 11 (1), 115. https://doi.org/10.1186/1475-2859-11-115.

Saripan, A.F., Reungsang, A., 2013. Biohydrogen production by *Thermoanaerobacterium thermosaccharolyticum* KKU-ED1: Culture conditions optimization using xylan as the substrate. Int. J. Hydrogen Energy 38 (14), 6167–6173. https://doi.org/10.1016/j.ijhydene.2012.12.130.

Sekoai, P.T., Ouma, C.N.M., du Preez, S.P., Modisha, P., Engelbrecht, N., Bessarabov, D. G., Ghimire, A., 2019. Application of nanoparticles in biofuels: An overview. Fuel 237, 380–397. https://doi.org/10.1016/j.fuel.2018.10.030.

Sheng, T., Gao, L., Zhao, L., Liu, W., Wang, A., 2015. Direct hydrogen production from lignocellulose by the newly isolated *Thermoanaerobacterium thermosaccharolyticum* strain DD32. RSC Adv. 5 (121), 99781–99788.

Sinha, P., Pandey, A., 2011. An evaluative report and challenges for fermentative biohydrogen production. Int. J. Hydrogen Energy 36 (13), 7460–7478. https://doi.org/10.1016/j.ijhydene.2011.03.077.

Srivastava, N., Srivastava, M., Malhotra, B.D., Gupta, V.K., Ramteke, P.W., Silva, R.N., Shukla, P., Dubey, K.K., Mishra, P.K., 2019. Nanoengineered cellulosic biohydrogen production via dark fermentation: A novel approach. Biotechnol. Adv. 37 (6), 107384. https://doi.org/10.1016/j.biotechadv.2019.04.006.

Tawfik, A., Nasr, M., Galal, A., El-Qelish, M., Yu, Z., Hassan, M.A., Salah, H.A., Hasanin, M.S., Meng, F., Bokhari, A., Qyyum, M.A., Lee, M., 2021. Fermentation-based nanoparticle systems for sustainable conversion of black-liquor into biohydrogen. J. Clean. Prod. 309, 127349. https://doi.org/10.1016/j.jclepro.2021.127349.

Vemuri, B., Xia, L., Chilkoor, G., Jawaharraj, K., Sani, R.K., Amarnath, A., Kilduff, J., Gadhamshetty, V., 2021. Anaerobic wastewater treatment and reuse enabled by thermophilic bioprocessing integrated with a bioelectrochemical/ultrafiltration module. Bioresour. Technol. 321, 124406. https://doi.org/10.1016/j.biortech.2020.124406.

Wang, J., Bibra, M., Venkateswaran, K., Salem, D.R., Rathinam, N.K., Gadhamshetty, V., Sani, R.K., 2018. Biohydrogen production from space crew's waste simulants using thermophilic consolidated bioprocessing. Bioresour. Technol. 255, 349–353. https://doi.org/10.1016/j.biortech.2018.01.109.

Wang, J., Wan, W., 2009. Factors influencing fermentative hydrogen production: A review. Int. J. Hydrogen Energy. 34 (2), 799–811. https://doi.org/10.1016/j.ijhydene.2008.11.015.

Xie, L.i., Yoshida, N., Ishii, S., Meng, L., 2021. Isolation and polyphasic characterization of *Desulfuromonas versatilis* sp. Nov., an electrogenic bacteria capable of versatile metabolism isolated from a graphene oxide-reducing enrichment culture. Microorganisms 9 (9), 1953. https://doi.org/10.3390/microorganisms9091953.

Zhang, T., Tremblay, P.-L., 2020. Graphene: An Antibacterial Agent or a Promoter of Bacterial Proliferation? iScience 23 (12), 101787. https://doi.org/10.1016/j.isci.2020.101787.